


RESEARCH ARTICLE

kcna1a mutant zebrafish model episodic ataxia type 1 (EA1) with epilepsy and show response to first-line therapy carbamazepine

Deepika Dogra^{1,2,3} | Paola L. Meza-Santoscoy^{1,2,3} | Cezar Gavrilovici^{1,2,3,4,5} |
 Renata Rehak^{1,2,3} | Cristiane L. R. de la Hoz^{1,2,3} | Kingsley Ibhazehiebo^{1,2,3} |
 Jong M. Rho^{1,2,3,4,5}  | Deborah M. Kurrasch^{1,2,3} 

¹Department of Medical Genetics, University of Calgary, Calgary, Alberta, Canada

²Alberta Children's Hospital Research Institute, University of Calgary, Calgary, Alberta, Canada

³Hotchkiss Brain Institute, University of Calgary, Calgary, Alberta, Canada

⁴Departments of Pediatrics, Clinical Neurosciences, Physiology & Pharmacology, Cumming School of Medicine, University of Calgary, Calgary, Alberta, Canada

⁵Departments of Neurosciences, Pediatrics, and Pharmacology, Rady Children's Hospital San Diego, University of California San Diego, San Diego, California, USA

Correspondence

Deborah M. Kurrasch, University of Calgary, 3330 Hospital Drive NW, HSC 2215, Calgary, AB T2N 4N1, Canada.
 Email: kurrasch@ucalgary.ca

Funding information

Brain Canada Platform Support Grant

Abstract

Objective: *KCNA1* mutations are associated with a rare neurological movement disorder known as episodic ataxia type 1 (EA1), and epilepsy is a common comorbidity. Current medications provide only partial relief for ataxia and/or seizures, making new drugs needed. Here, we characterized zebrafish *kcna1a*^{-/-} as a model of EA1 with epilepsy and compared the efficacy of the first-line therapy carbamazepine in *kcna1a*^{-/-} zebrafish to *Kcna1*^{-/-} rodents.

Methods: CRISPR/Cas9 mutagenesis was used to introduce a mutation in the sixth transmembrane segment of the zebrafish *Kcna1* protein. Behavioral and electrophysiological assays were performed on *kcna1a*^{-/-} larvae to assess ataxia- and epilepsy-related phenotypes. Real-time quantitative polymerase chain reaction (qPCR) was conducted to measure mRNA levels of brain hyperexcitability markers in *kcna1a*^{-/-} larvae, followed by bioenergetics profiling to evaluate metabolic function. Drug efficacies were tested using behavioral and electrophysiological assessments, as well as seizure frequency in *kcna1a*^{-/-} zebrafish and *Kcna1*^{-/-} mice, respectively.

Results: Zebrafish *kcna1a*^{-/-} larvae showed uncoordinated movements and locomotor deficits, along with scoliosis and increased mortality. The mutants also exhibited impaired startle responses when exposed to light-dark flashes and acoustic stimulation as well as hyperexcitability as measured by extracellular field recordings and upregulated *fosab* transcripts. Neural *vglut2a* and *gad1b* transcript levels were disrupted in *kcna1a*^{-/-} larvae, indicative of a neuronal excitatory/inhibitory imbalance, as well as a significant reduction in cellular respiration in *kcna1a*^{-/-}, consistent with dysregulation of neurometabolism. Notably, carbamazepine suppressed the impaired startle response and brain hyperexcitability in *kcna1a*^{-/-} zebrafish but had no effect on the seizure frequency

[Correction added on 27 June 2023 after first online publication: The title was updated to include the word 'show'.]

This is an open access article under the terms of the [Creative Commons Attribution-NonCommercial-NoDerivs](https://creativecommons.org/licenses/by-nc-nd/4.0/) License, which permits use and distribution in any medium, provided the original work is properly cited, the use is non-commercial and no modifications or adaptations are made.

© 2023 The Authors. *Epilepsia* published by Wiley Periodicals LLC on behalf of International League Against Epilepsy.

in *Kcna1*^{-/-} mice, suggesting that this EA1 zebrafish model might better translate to humans than rodents.

Significance: We conclude that zebrafish *kcna1a*^{-/-} show ataxia and epilepsy-related phenotypes and are responsive to carbamazepine treatment, consistent with EA1 patients. These findings suggest that *kcna1*^{-/-} zebrafish are a useful model for drug screening as well as studying the underlying disease biology.

KEYWORDS

carbamazepine, epilepsy, episodic ataxia type 1, KCNA1, zebrafish

1 | INTRODUCTION

Mutations in the *KCNA1* gene, encoding voltage-gated potassium channel α -subunit Kv1.1, are associated with episodic ataxia type 1 (EA1). The usual onset of EA1 occurs in childhood or early adolescence, and patients often experience multiple episodes on daily basis.¹ EA1 is characterized by myokymia and spastic contractions of skeletal muscles of the head and limbs along with loss of motor coordination and balance. Some patients with EA1 may also encounter focal-onset epilepsy, delayed motor development, and cognitive disability. Episodes of discoordination in EA1 are usually triggered by stressors, including startle, emotional stress, exercise, and temperature.^{2,3} Some individuals with mutations in *KCNA1* also have skeletal deformities including scoliosis, kyphoscoliosis, high arched palate, and minor craniofacial dysmorphism.^{4,5}

KCNA1 is highly expressed in interneurons, particularly the basket cells of the cerebellum, where it forms inhibitory γ -aminobutyric acid (GABA)ergic synapses onto Purkinje cells. Mechanistically, KCNA1 plays an important role in the repolarization phase of presynaptic action potentials that provides the inhibitory inputs to Purkinje cells. Thus, *KCNA1* mutations result in the hyperexcitability of the presynaptic basket cells and the excessive release of GABA neurotransmitter, which can inhibit the generation of action potentials. As a consequence, the inhibitory output of the cerebellum may be markedly reduced, thus causing hyperexcitability and cerebellar symptoms observed in patients with EA1.⁶

The current therapeutic strategy for KCNA1-related EA1 is treatment with the carbonic anhydrase inhibitor acetazolamide, which provides partial symptomatic relief by reducing the frequency of ataxic episodes in some individuals. However, long-term side effects of acetazolamide include chronic metabolic acidosis, kidney stones, neuropsychiatric manifestations, fatigue, and paresthesias.^{2,7}

Phenytoin, a blocker of voltage-gated sodium channels is also effective in EA1 patients; however, its potential to induce permanent cerebellar dysfunction and atrophy has

Key points

- Zebrafish *kcna1a*^{-/-} larvae display dynamic behavioral changes, along with ataxia-like uncoordinated movements and brain hyperexcitability.
- *kcna1a*^{-/-} larvae have dysfunctional neuronal excitatory/inhibitory balance and perturbed metabolic health.
- Carbamazepine treatment improves behavioral deficits and brain hyperexcitability in *kcna1a*^{-/-} larvae.

raised concerns against its long-term use.⁷ Instead, carbamazepine is a related sodium channel blocker that can partially relieve ataxia and seizures in a patient subpopulation with fewer concerns for long-term use.⁸⁻¹⁰ Of note, twins with a shared *KCNA1* mutation and epileptic phenotypes of different severity revealed that although lamotrigine controlled the convulsive episodes in one child, the other twin had drug-resistant seizures,¹¹ demonstrating the challenges of treating this disorder. Combined, current medications fail to provide effective treatment for the ataxia and seizures, making animal models necessary to provide further insights into the cellular and molecular mechanisms of the disorder as well as to enable future drug screening.

In murine models of EA1, loss-of-function of KCNA1 causes an increase in GABA release, thereby inhibiting Purkinje cells in the cerebellum and ultimately leading to ataxia.^{12,13} Furthermore, in support of an epileptogenic role for *KCNA1* mutations, *Kcna1*^{-/-} mice exhibit epileptic phenotypes similar to patients, such as recurrent spontaneous seizures including myoclonic and generalized tonic-clonic seizures that begin 3–4 weeks postnatally.^{14,15} *Kcna1*^{-/-} mice also exhibit cardiorespiratory dysfunction and sudden unexpected death in epilepsy.¹⁶⁻¹⁹ However, *Kcna1*^{-/-} mice have limited utility for drug screening given their expense and the inability to conduct primary high-throughput screening in rodents. A cheaper model

of EA1 is needed to initiate the large-scale drug screening required to discover better treatment options.

Zebrafish are commonly used to model human neurological disorders given that they are vertebrates and display high molecular and cellular homology with human brain. In addition, larval and adult zebrafish display well-established and stereotypical behaviors that can be easily analyzed, which is especially helpful when modeling movement disorders. Thus, to explore the phenotypes related to EA1 with epilepsy due to loss of *KCNA1*, we generated a genetic mutant of one of the zebrafish paralogs *kcna1a*, expressed in reticulospinal neurons that regulate the animal's startle response. We performed a comprehensive analysis of *kcna1a* homozygous mutants (hereafter addressed as *kcna1a*^{-/-}) to obtain better insights into the behavioral, electrophysiological, molecular, and metabolic consequences of *Kcna1* dysfunction.

2 | MATERIALS AND METHODS

2.1 | Zebrafish husbandry

All protocols and procedures were approved by the Health Science Animal Care Committee (protocol number AC22-0153) at the University of Calgary in compliance with the Guidelines of the Canadian Council of Animal Care. Adult wild-type zebrafish (TL strain) were maintained at 28°C in a 14-h light/10-h dark cycle under standard aquaculture conditions, and fertilized eggs were collected via natural spawning. The animals were fed twice daily with Artemia. Zebrafish embryos and larvae were maintained in a non-CO₂ incubator (VWR) at 28°C on the same light-dark cycle as the aquatic facility.

2.2 | Generation of zebrafish mutants

kcna1a^{ca201/ca201} (*kcna1a*^{-/-}) zebrafish were generated by using CRISPR/Cas9 mutagenesis. The identified founder carried a six nucleotide deletion within the second exon (gRNA sequence: GGTTCCTGTGCGCCATCGCTGG), producing a two amino acid deletion (Ile, Ala). The F1 heterozygous animals were outcrossed with wild-types to raise F2 adults, which were used in the experiments. Genotyping was carried out by performing PCR using primers: *kcna1a*_F-GACCCTCAAAGCCAGTATGCG and *kcna1a*_R-GACTTGCTGACGGTTGAGGAG, followed by restriction digestion using BtgZI (NEB, R0703S). All three genotypes were distinguished by running the digested PCR product on a gel, based on different patterns and sizes of PCR product bands (wild-types: two bands- 214 and 191 bp; heterozygotes: three bands- 399, 214, and

191 bp; homozygotes: one band- 399 bp). All the morphological analysis, including the eye and head size measurements were performed using ZEN software (ZEISS). Movies of freely swimming larvae were recorded using Stereo Discovery.V8 microscope (ZEISS).

2.3 | Gene expression analysis by in situ hybridization and real-time qPCR

Digoxigenin-labeled probes were synthesized for *kcna1a* as described previously²⁰ using the following primers: *kcna1a*_insitu_F- CTCTGCCGTGCCGGGGCAT and *kcna1a*_insitu_R- CAATGTTCCGGTTGCTCACG. The embryos and larvae were fixed at requisite stage in 4% paraformaldehyde (Sigma-Aldrich) overnight at 4°C. The whole mount in situ hybridization protocol used was the same as described previously.²⁰

fosab, *vglut2a*, and *gad1b* real-time quantitative polymerase chain reaction (qPCR) was performed on cDNA obtained from the heads of 3 day post fertilization (dpf) and 5 dpf larvae. *kcna1a* and *kcna1b* qPCR were performed on cDNA obtained from the heads of 3 dpf larvae. *rpl13* was used as internal control. The following primers were used for qPCR: *rpl13*_qPCR_F- TAAGGACGGAGTGAACAACCA and *rpl13*_qPCR_R- CTTACGTCTGCGGATCTTTCTG; *kcna1a*_qPCR_F- GATAGTGCGCTTCTTGCTTGC and *kcna1a*_qPCR_R- GCCCTTCCCTCTTTCCGTC; *kcna1b*_qPCR_F- GAGTTGATCGTCCGCTTCTTC and *kcna1b*_qPCR_R- CTTCCCGCCTTCGGGATC; *fosab*_qPCR_F-TCGACGTGAACTCA CCGATA and *fosab*_qPCR_R-CTTGCAGATGGGTT TGTGTG; *gad1b*_qPCR_F- AACTCAGGCGATTGTTGCA and *gad1b*_qPCR_R- TGAGGACATTTCCAGCCTTC; *vglut2a*_qPCR_F- CATCCTGTCTACAACACTACGGTT and *vglut2a*_qPCR_R- CCAACACCAGAAATGAAATAGCCA.

2.4 | Live alizarin red staining

Twelve dpf larvae were incubated for 4 h in 40 mL of system water containing 500 µL of 0.2% alizarin red stock solution (Sigma) at 28°C. The stained fish were washed in system water overnight and imaged the next day (13 dpf) using the LSM 900 confocal microscope (ZEISS). The thickness of six vertebral segments was measured using ZEN software (ZEISS) and the average was plotted (GraphPad Prism).

2.5 | Behavioral assays

Five dpf zebrafish larvae maintained in 48-well plates were habituated for 20 min, under ambient light. This was

followed by behavioral assessment to measure distance moved under various environmental conditions (100% light, light–dark flashes, acoustic startle) in Zebrafish (Viewpoint Life Sciences). Tracking of total distance moved as a measure of swimming behavior was analyzed using Zebrafish V3 software (Viewpoint Life Sciences). Distance traveled and time taken were retrieved from behavioral data to calculate speed.

2.6 | Drug treatment

Carbamazepine (Cayman Chemical), acetazolamide (Santa Cruz Biotechnology), phenytoin (Santa Cruz Biotechnology), and lamotrigine (Cayman Chemical) stock solutions were prepared in dimethyl sulfoxide (DMSO). On the day of behavioral assays, the stock solutions were diluted to a final concentration of 50 μ M in embryo media. The zebrafish larvae were treated with 50 μ M drugs for 2h, followed by behavioral assessments. The final DMSO concentration was 0.5% and was used as vehicle control in behavioral assays.

For implant surgery and mouse video-EEG (electroencephalography), carbamazepine was dissolved in DMSO to a final concentration of 40 mg/kg body weight. Vehicle solution used was 10% DMSO.

2.7 | Metabolic measurements

Oxygen consumption rate (OCR) measurements were performed using the XF24 Extracellular Flux Analyzer (Seahorse Biosciences). Single 3 dpf and 6 dpf zebrafish larvae were placed in 24 wells on an islet microplate and an islet plate capture screen was placed over the measurement area to maintain the larvae in place. Seven measurements were taken to establish basal rates, followed by treatment injections and 18 additional cycles.²¹ Rates were determined as the mean of two measurements, each lasting 2 min, with 3 min between each measurement.²² Three independent assays were performed to establish metabolic measurements.

2.8 | Electrophysiological measurements

Electrophysiological recordings in zebrafish larvae were performed as described previously.^{23,24} Briefly, 3 dpf zebrafish were paralyzed using α -bungarotoxin (1 mg/mL, Tocris) and embedded in 1.2% low melting-point agarose. The dorsal side of the zebrafish was exposed to the agarose gel surface and accessible for electrode

placement. Larvae zebrafish were placed on an upright stage of a Zeiss Axioskop2 microscope, visualized using a 5X Zeiss N-Achroplan objective, and perfused with embryo media. A glass microelectrode (3–8 M Ω) filled with 2 M NaCl was placed into the optic tectum of zebrafish, and a recording was performed in current-clamp mode, low-pass filtered at 1 kHz, high-pass filtered at 0.1 Hz, using a digital gain of 10 (Multiclamp 700B amplifier, Digidata 1440A digitizer, Axon Instruments) and stored on a PC computer running pClamp software (Axon Instruments). Baseline recording was performed for 30 min. For carbamazepine testing, after 5 min of baseline recording, carbamazepine (50 μ M) was perfused into the bath for 10 min followed by 30-min recording. The larvae were exposed to carbamazepine for a total of 40 min. The threshold for detection of spontaneous events was set at three times noise, as described previously.²⁵ The frequency and amplitude of spontaneous events were analyzed using the Clampfit software 11.0.3 (Molecular Devices, Sunnyvale, CA).

2.9 | Implant surgery and mouse video-EEG

Kcna1-null mice were anesthetized with 3% isoflurane, and the skull fixated with stereotaxic bars (KOPF Instruments) over heating pads (as approved in Animal protocol # AC21-0164). A 1.5 cm rostral-caudal incision was made to expose the skull surface, and connective tissues cleared. Three holes were gently drilled on each side of the skull with a 23 mm gauge needle, avoiding suture lines. Mouse screws (0.1 inch) with wire leads were gently inserted midway into the skull, and a layer of dental acrylic was applied over the screw heads and skull. A 6-pin mouse connector (Pinnacle Technology) was positioned over the screws, and wires properly aligned, wrapped together, and folded backwards to avoid accidental contacts. A pocket for two EMG electrodes was made in the neck of the mouse by blunt dissection. Exposed wires were covered with a final layer of dental acrylic, and allowed to harden for 24h before attaching the pin connector to the video-EEG monitor (Pinnacle Technology). EEG signals were recorded simultaneously across the rostral, medial, and caudal aspects of the neocortex using Sirenia Acquisition software (Pinnacle Technology). Mice were recorded 24h per day for 1 day (baseline, postnatal day, P36–38), and received carbamazepine (intraperitoneal injection, 40 mg/kg body weight/day) for the next six consecutive days (P39–44). Frequency, duration, and time of seizure was analyzed using Sirenia Seizure software (Pinnacle Technology).

2.10 | Statistical analysis

GraphPad Prism 9.4.1 was used to perform statistical analysis. Data are represented as mean \pm SEM. *p*-values were calculated by unpaired *t* test.

3 | RESULTS

3.1 | *kcn1a* mRNA expression in wild-type and morphological analyses of *kcn1a*^{-/-} larvae

Due to a genome duplication event millions of years ago, zebrafish possess two paralogs of *KCNA1*, that is, *kcn1a* and *kcn1b*. Zebrafish *kcn1a* (but not *kcn1b*) is expressed in the Mauthner (M) cells that are a type of reticulospinal neurons (RSNs) in the hindbrain, contributing to neuronal firing and rapid startle behavior in response to external stimuli. *kcn1a* expression is also detected in two M cell homologs, MiD2cm and MiD3cm, involved in repetitive firing.^{26,27} Here, we performed in situ hybridization to further confirm the *kcn1a* mRNA expression in

the M cells in hindbrain at 2 dpf and 5 dpf, as well as in the RSNs in midbrain (nucleus of the medial longitudinal fasciculus nMLF) and neurons in the spinal cord at 5 dpf (Figure 1A).

Next, we injected a CRISPR targeting the second exon of *kcn1a* gene to generate a *kcn1a* mutant allele, *kcn1a*^{-/-}. The mutation led to a six-nucleotide deletion, causing a two amino acid deletion in the sixth transmembrane segment (S6) of the Kcn1a protein, which is conserved among humans, mice, and zebrafish (Figure 1B–D). Notably, mutations in the conserved Pro-Val-Pro motif in S6 are linked to epileptic encephalopathy.^{11,28} As assessed by qPCR, *kcn1a* transcript levels were significantly reduced in *kcn1a*^{-/-} compared to wild-type siblings (WTs) at 3 dpf (Figure 1E), suggesting active mRNA degradation of mutant transcripts. No significant changes were observed in *kcn1b* transcript levels in the *kcn1a*^{-/-} compared to WTs at 3 dpf, indicating a lack of genetic compensation by this paralog in the mutant background (Figure S1A). Morphological analyses revealed no significant differences between *kcn1a*^{-/-} larvae and WTs at 3 dpf (Figure S1B). However, at 6 dpf, *kcn1a*^{-/-} larvae exhibited a 13% reduction in

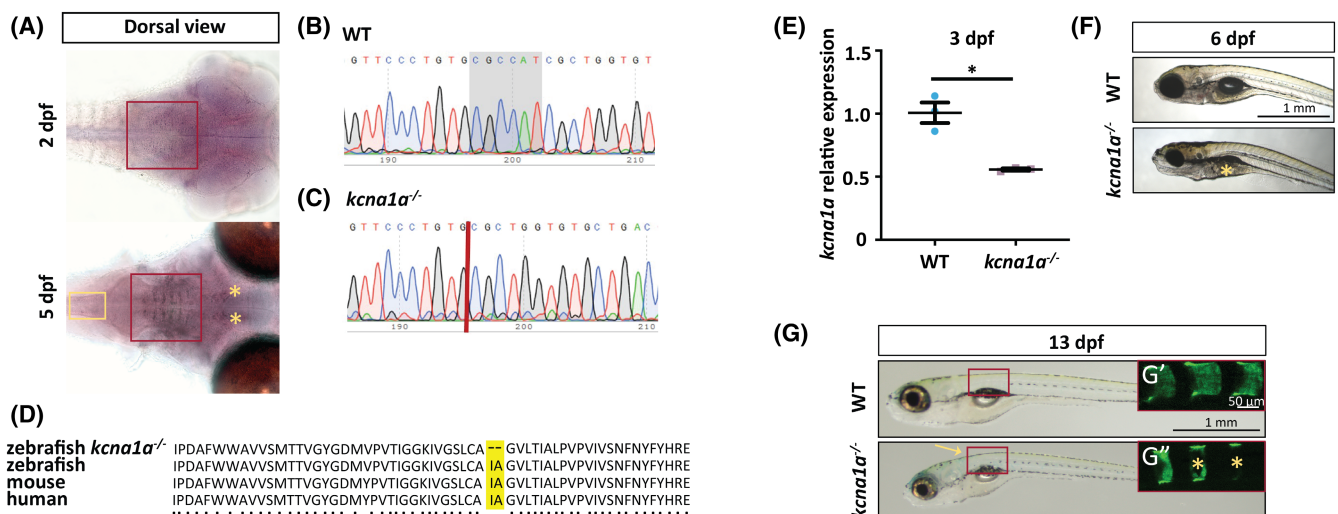


FIGURE 1 Expression analysis of *kcn1a* and generation of *kcn1a*^{-/-} zebrafish model using CRISPR/Cas9 technique. (A) In situ hybridization for *kcn1a* expression at 2 dpf and 5 dpf. Red boxes indicate RNA probe signal in M cells in hindbrain at 2 dpf and 5 dpf. Yellow asterisks indicate RNA probe signal in nMLF in midbrain at 5 dpf. Yellow box indicates RNA probe signal in the neurons present in the spinal cord at 5 dpf. (B, C) Nucleotide sequences of *kcn1a* in zebrafish WT and *kcn1a*^{-/-}. Gray highlighted region indicates the six nucleotides deleted due to mutation in *kcn1a*^{-/-}. (D) Amino acid sequence of Kcn1a in zebrafish *kcn1a*^{-/-} and WT, and orthologues in mouse (KCNA1) and human (KCNA1). Yellow highlighted region indicates two amino acid deletions due to mutation in *kcn1a*^{-/-}. (E) qPCR analysis for relative *kcn1a* mRNA expression in 3 dpf *kcn1a*^{-/-} larvae compared to WT. WT and *kcn1a*^{-/-}, *n* = 3 × 10 larvae assessed as three biological and two technical replicates each. *kcn1a* is downregulated in *kcn1a*^{-/-} indicating active mRNA degradation. (F) WT and *kcn1a*^{-/-} larvae at 6 dpf. Yellow asterisk indicates absence of swim bladder in *kcn1a*^{-/-} larvae. (G, G', G'') WT and *kcn1a*^{-/-} larvae at 13 dpf. Yellow arrow points to spinal curvature progression in *kcn1a*^{-/-} larvae. Red boxes outline the trunk regions with alizarin red stained vertebral segments (G', G''). Yellow asterisks indicate missing or deformed vertebral segments in *kcn1a*^{-/-} larvae. Scale bars = 1 mm, 50 μm. Data are mean \pm SEM, **p* ≤ .05. Unpaired *t* test. dpf, days post fertilization; M cells, Mauthner cells; nMLF, nucleus of the medial longitudinal fasciculus; WT, wild-type.

eye diameter compared to WT, with no significant difference in head size (Figure S1C,D). This reduction in eye size is perhaps related to the vision defects reported in KCNA1-deficient patients.²⁹ Notably, ~55% of 6 dpf *kcna1a*^{-/-} larvae did not inflate their swim bladder, indicating developmental delay (Figure 1F, Figure S1E). We further assessed the mutant larvae as they aged and observed a spinal curve progression at ~13 dpf (Figure 1G, white arrow). We next performed alizarin staining on live larvae to assess vertebral segment abnormalities and related skeletal deformation. At 13 dpf, compared to WT, some of the vertebral segments in the mutants were either missing or not fully formed (Figure 1G',G''), with an ~26% overall reduction in their thickness (Figure S1F). Thus, our *kcna1a*^{-/-} larvae also exhibit scoliosis-like defects as reported previously in certain KCNA1-deficient patients.⁴ Furthermore, the homozygous mutants survive until 14 dpf (Figure S1G),

whereas the heterozygotes live into adulthood and breed well (data not shown).

3.2 | *kcna1a*^{-/-} larvae exhibit locomotor deficits and movement disorders

Zebrafish models of epilepsy exhibit behavioral comorbidities similar to those observed in individuals with epilepsy.³⁰ To ascertain the effect of *kcna1a* mutation on larval zebrafish behavior, we assessed larval swimming activity at 3 dpf and 5 dpf for 30 min in the light. Of note, wild-type zebrafish larvae show higher levels of active swimming as they get older, since they have a fully inflated swim bladder, thus we observe higher distance traveled by 5 dpf WT, compared to 3 dpf. The total distance traveled and the speed of 3 dpf *kcna1a*^{-/-} larvae were significantly higher compared to WT (Figure 2A,B). The

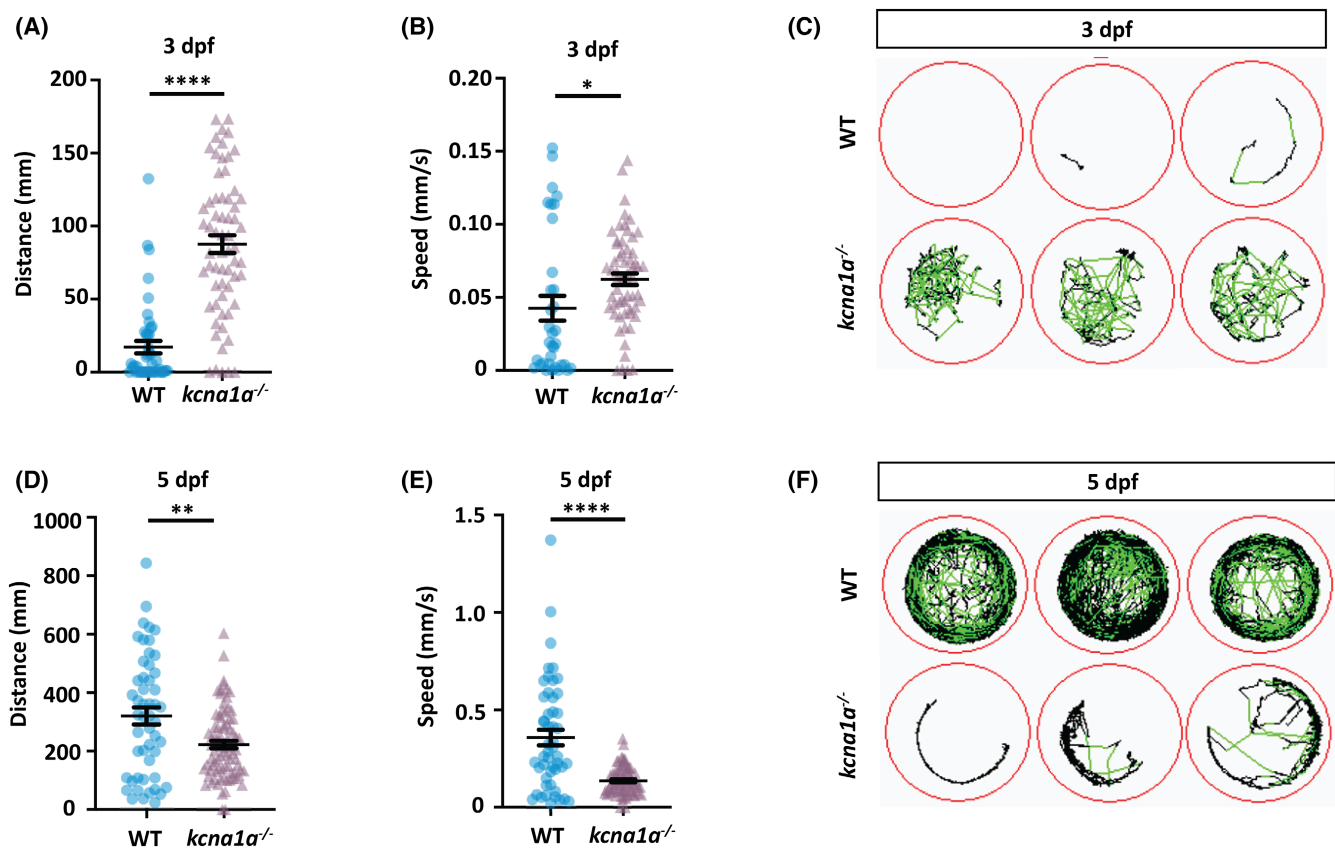


FIGURE 2 Spontaneous behavior analysis of *kcna1a*^{-/-} zebrafish. (A) Quantification of distance traveled at 3 dpf tracked in 100% light for 30 min. *kcna1a*^{-/-} move higher distances compared to WT. WT, *n* = 44; *kcna1a*^{-/-}, *n* = 63. (B) Quantification of speed at 3 dpf tracked in 100% light for 30 min. Speed of *kcna1a*^{-/-} is significantly higher than WT. WT, *n* = 34; *kcna1a*^{-/-}, *n* = 60. (C) Locomotor plots at 3 dpf, showing that *kcna1a*^{-/-} are more active than WT. WT, *n* = 20; *kcna1a*^{-/-}, *n* = 20. (D) Quantification of distance traveled at 5 dpf tracked in 100% light for 30 min. Distance traveled by *kcna1a*^{-/-} is significantly reduced compared to WT. WT, *n* = 51; *kcna1a*^{-/-}, *n* = 84. (E) Quantification of speed at 5 dpf tracked in 100% light for 30 min. Speed of *kcna1a*^{-/-} is significantly reduced compared to WT. WT, *n* = 50; *kcna1a*^{-/-}, *n* = 84. (F) Locomotor plots at 5 dpf, showing that *kcna1a*^{-/-} are moving less and have abnormal swimming patterns. WT, *n* = 20; *kcna1a*^{-/-}, *n* = 24. Data are mean ± SEM, **p* ≤ .05, ***p* ≤ .01, *****p* ≤ .0001- Unpaired *t* test.

locomotor traces of 3 dpf *kcna1a*^{-/-} larvae illustrate this hyperactivity compared to WT, which swim little during this earlier developmental stage (Figure 2C). Conversely, when assessed at 5 dpf, *kcna1a*^{-/-} larvae swam significantly shorter distances and with decreased speed compared to WT (Figure 2D,E). The locomotor traces further show the extent of this hypoactivity and uncoordinated movement patterns, a sign of ataxia, in 5 dpf *kcna1a*^{-/-} larvae (Figure 2F). We further analyzed the pattern of swimming trajectory in 5 dpf mutants by recording movies and confirmed that their swimming pattern was abnormal compared to WT (Movies S1 and S2). Together, these results illustrate the dynamic changes in swimming

behaviors of *kcna1a*^{-/-} larvae across development and the appearance of their ataxia-like features at a later age.

3.3 | *kcna1a*^{-/-} larvae exhibit impaired startle response that is rescued by carbamazepine treatment

Because convulsions in EA1 patients can be triggered by extrinsic stimuli, we assessed the response of *kcna1a*^{-/-} larvae to different environmental triggers. We tested an acoustic startle protocol on 5 dpf larvae for 10 min by introducing vibration pulses of 440 Hz in the light (Figure 3A)

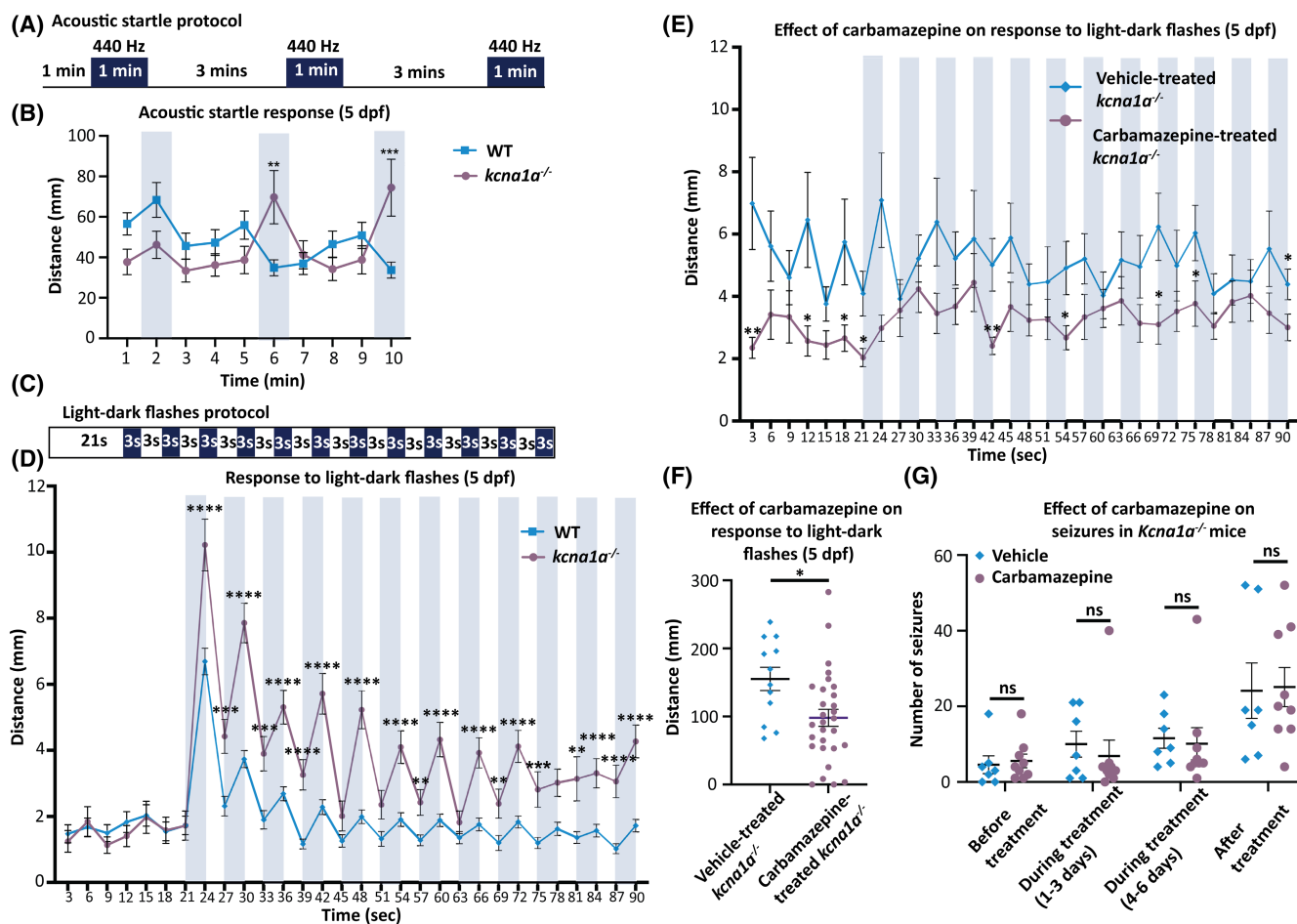


FIGURE 3 Analysis of startle response in *kcna1a*^{-/-} zebrafish and effect of carbamazepine treatment on *kcna1a*^{-/-} zebrafish and *Kcna1a*^{-/-} mice. (A) Schematic representation of acoustic startle protocol. (B) Quantification of distance traveled every 1 min in acoustic startle at 5 dpf. *kcna1a*^{-/-} are more responsive to startle with significantly higher distance traveled in second and third vibration pulse compared to WT. WT, *n* = 113; *kcna1a*^{-/-}, *n* = 52. (C) Schematic representation of light–dark flashes protocol. (D) Quantification of distance traveled every 3 s in light–dark flashes at 5 dpf. *kcna1a*^{-/-} show higher sensitivity to startle with more distance traveled compared to WT. WT, *n* = 108; *kcna1a*^{-/-}, *n* = 63. (E, F) Quantification of distance traveled every 3 s (E) and in 90 s (F) in light–dark flashes after treatment with carbamazepine at 5 dpf. Carbamazepine treatment rescues impaired startle response in *kcna1a*^{-/-}. Vehicle-treated *kcna1a*^{-/-}, *n* = 12; carbamazepine-treated *kcna1a*^{-/-}, *n* = 29. (G) Quantification of number of seizures encountered by vehicle- and carbamazepine-treated P36–38 *Kcna1a*^{-/-} mice at different time points. Carbamazepine treatment does not reduce the frequency of seizures in *Kcna1a*^{-/-} mice. Vehicle-treated *Kcna1a*^{-/-}, *n* = 7; carbamazepine-treated *Kcna1a*^{-/-}, *n* = 9. Data are mean ± SEM, ns: no significant changes observed, **p* ≤ .05, ***p* ≤ .01, ****p* ≤ .001, *****p* ≤ .0001- Unpaired *t* test.

and calculated the total distance traveled at the end of every 1 min. The *kcn1a*^{-/-} larvae moved significantly longer distances during the second and third pulses compared to WTs, consistent with an abnormal response to acoustic startle (Figure 3B), as well as a recent study.³¹ We also performed a protocol of 3 s light–dark flashes on 5 dpf larvae for a total duration of 90 s (Figure 3C) and measured the total distance traveled at the end of every 3 s. The *kcn1a*^{-/-} larvae showed an exaggerated response to light–dark flashes and traveled longer distances compared to WTs (Figure 3D).

Next, we examined whether the impaired startle behavior of our *kcn1a*^{-/-} zebrafish larvae was improved by treatment with carbamazepine, a sodium channel blocker that can reduce seizures in patients with KCNA1-related epilepsy.⁸ We ran the light–dark flashes protocol (as described above) on untreated animals and sorted the 5 dpf *kcn1a*^{-/-} larvae into two bins: those with a total distance traveled <100 mm and those with a total distance traveled ≥100 mm (Figure S2A). We collected the 5 dpf *kcn1a*^{-/-} larvae with ≥100 mm distance traveled and treated with carbamazepine (50 μM) or DMSO (vehicle-control; 0.5%) for 2 h, followed by the same light–dark flashes protocol (as described above) to assess the distance traveled ± drug. Notably, this dose was selected by titrating carbamazepine to identify the concentration that did not significantly affect the swimming activity of WTs (Figure S2B). Carbamazepine treatment rescued the impaired startle response in *kcn1a*^{-/-} larvae, since the distance traveled every 3 s was significantly lower at several time-points and the total distance swam during the complete protocol of 90 s was reduced by ~37% (Figure 3E,F). We further assessed the effect of other anti-seizure medications used in EA1 patients, including acetazolamide, phenytoin, and lamotrigine, on the impaired startle response in *kcn1a*^{-/-} larvae.^{7,11} We treated 5 dpf *kcn1a*^{-/-} larvae (after sorting as described above) with 50 μM of each of these compounds and DMSO (vehicle-control; 0.5%) for 2 h and performed the light–dark flashes protocol (as described above) to assess the distance traveled. Acetazolamide, phenytoin, and lamotrigine treatments rescued the impaired startle response in *kcn1a*^{-/-} larvae, since the total distance swam during the complete protocol of 90 s was reduced by ~63%, ~74%, and ~62%, respectively (Figure S2C). Again, the concentration of each drug was decided by titration to identify the concentration that did not significantly affect the swimming activity of WTs (Figure S2D). Of note, the movement of our *kcn1a*^{-/-} larvae is sensitive to the time of the day the behavior assessments were performed. We showed that the distance traveled in 5 min in the light by 5 dpf *kcn1a*^{-/-} larvae at 12 pm is significantly higher than at 9 am (Figure S2E). Thus,

all behavior assessments in this study are performed at 9 am on untreated larvae for the sorting protocol and at 12 pm following a 2-h drug/vehicle treatment, including the appropriate controls at each time point. Combined, *kcn1a*^{-/-} zebrafish respond positively to the same drug treatments used in EA1 patients.

Mouse models are traditionally favored over zebrafish for translational studies and thus we wanted to compare the efficacy of carbamazepine in *kcn1a*^{-/-} zebrafish to its effects in *Kcna1*^{-/-} mice that display spontaneous recurrent seizures beginning between P21 and P28 that become more severe and frequent with age. Previous studies using *Kcna1* knockout mice show that carbamazepine partially reduces seizure frequency but is ineffective against severe seizures.^{32,33} We treated epileptic P36–38 *Kcna1*^{-/-} mice with carbamazepine (40 mg/kg) or DMSO (vehicle-control; 10%) and quantified the number of seizures per day with video-EEG recordings across an early-, late-, and post- treatment window (Figure 3G). Carbamazepine treatment had no effect on seizure frequency in *Kcna1*^{-/-} mice, indicating that at least for this drug, the zebrafish larvae response is more in alignment with *KCNA1* patients than mice.

3.4 | *kcn1a*^{-/-} larvae exhibit brain hyperexcitability that is rescued by carbamazepine treatment

Similar to mice, zebrafish epilepsy models display neuronal hyperexcitability in electrophysiological recordings.^{23,24} Thus, we wanted to test the effects of a *kcn1a* mutation on brain hyperactivity, as a proxy for an epileptic state. We measured extracellular field potentials from the optic tectum of agarose-immobilized 3 dpf WTs and *kcn1a*^{-/-} larvae brains (Figure S3A). WTs (Figure 4A) and *kcn1a*^{+/-} (Figure S3B) showed no evidence of abnormal electrical activity; however, extracellular field recordings in ~60% of *kcn1a*^{-/-} larvae revealed repetitive inter-ictal like discharges (<1 s duration) with high-frequency, large-amplitude spikes (1.6 ± 0.5 Hz; 0.4 ± 0.1 mV, mean ± SEM), consistent with a spontaneous epileptic phenotype (Figure 4B,B'). Of interest, longer duration (>1 s) discharges (2.8 ± 0.3 s; 0.28 ± 0.001 mV; mean ± SEM) characterized as ictal-like events³⁴ were also identified in ~13% of *kcn1a*^{-/-} larvae (Figure S3C). The limited number of ictal-like events identified in the mutant larvae might be linked to the early larval stage (3 dpf) at which the recordings were performed. We speculate that the ictal-like events in *kcn1a*^{-/-} larvae would become more prominent between 4 and 7 dpf, in a manner similar to that described for a zebrafish model of Dravet syndrome.³⁴ We next wanted to assess the effect of carbamazepine treatment

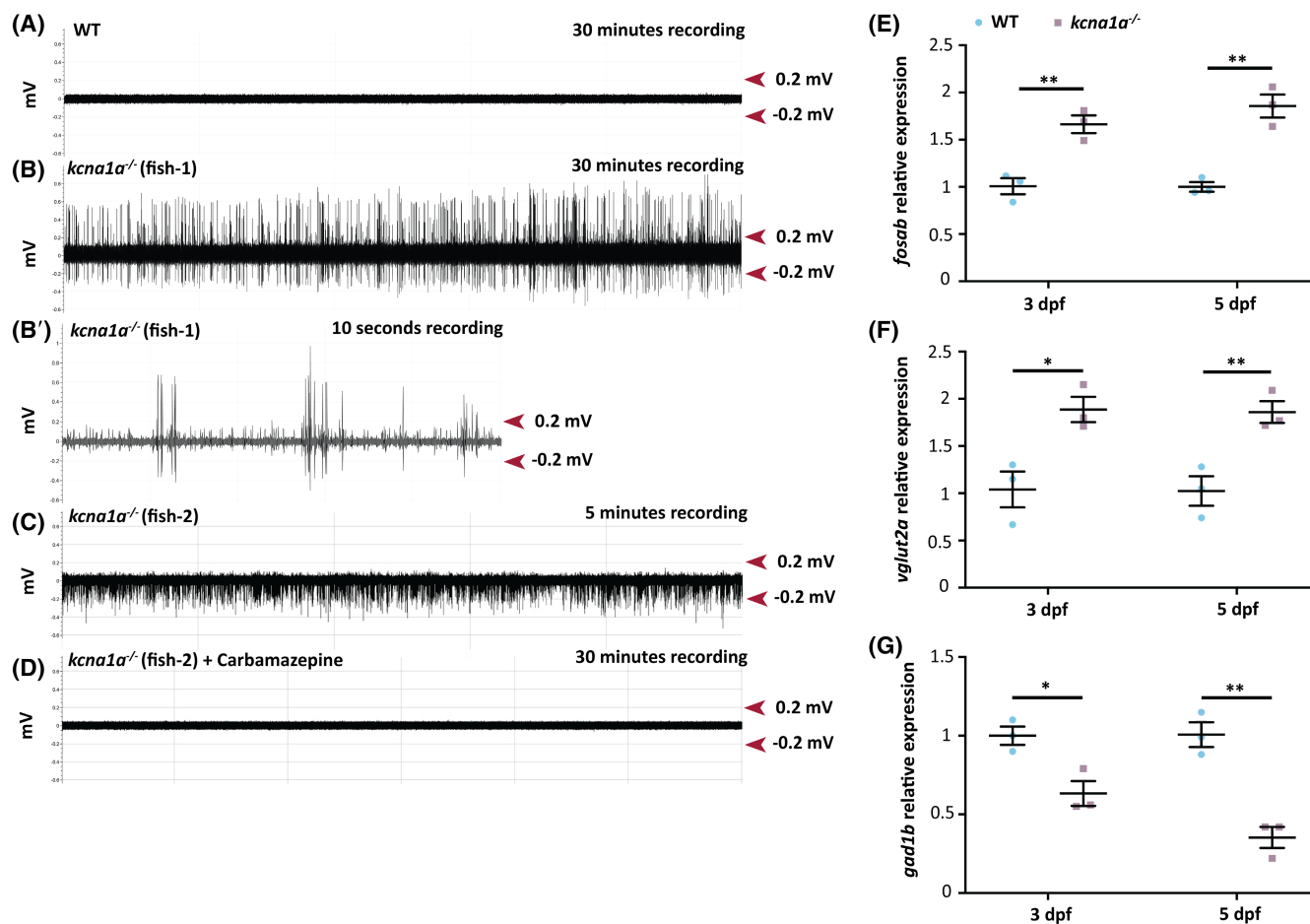


FIGURE 4 Brain hyperexcitability and E/I imbalance analysis in *kcna1a*^{-/-} zebrafish. (A, B, B') Representative extracellular field recordings obtained from the optic tectum of 3 dpf WT (A) and *kcna1a*^{-/-} zebrafish larvae (B, B' - higher magnification of B). WTs show no evidence of abnormal electrical activity. The repetitive inter-ictal like discharges with high-frequency large amplitude spikes (1.6 ± 0.5 Hz; 0.4 ± 0.1 mV) seen in the *kcna1a*^{-/-} are indicative of increased network hyperexcitability. WT, $n = 7$ out of 7 with no abnormal activity; *kcna1a*^{-/-}, $n = 5$ out of 8 show epileptiform activity. (C, D) Representative extracellular recordings obtained from optic tectum of 3 dpf *kcna1a*^{-/-} zebrafish larvae before (C) and after treatment with carbamazepine (D). Carbamazepine treatment leads to the reversal of epileptiform activity of *kcna1a*^{-/-}. *kcna1a*^{-/-}, $n = 3$ out of 3 have their hyperexcitability rescued by carbamazepine. (E-G) qPCR analysis for relative *fosab*, *vglut2a*, and *gad1b* mRNA expression in 3 dpf and 5 dpf *kcna1a*^{-/-} larvae compared to WT. WT and *kcna1a*^{-/-}, $n = 3 \times 10$ larvae assessed as three biological and two technical replicates each. *fosab* is upregulated in *kcna1a*^{-/-} indicating brain hyperexcitability. *vglut2a* is upregulated and *gad1b* is downregulated in *kcna1a*^{-/-} indicating dysfunctional E/I balance. Data are mean \pm SEM, ns: no significant changes observed, * $p \leq .05$, ** $p \leq .01$ - Unpaired *t* test.

on the electrical hyperexcitability exhibited by our *kcna1a*^{-/-} larvae, and thus after the baseline recording, we perfused carbamazepine (50 μ M) into the bath and continued recording. One hundred percent of *kcna1a*^{-/-} larvae displaying electrical hyperexcitability had normalized epileptiform activity to WT levels following carbamazepine treatment (Figure 4C,D, Figure S3C,D). Notably, both inter-ictal like and ictal-like discharges exhibited by the mutants were reversed by this drug.

Because seizure induction in a rodent model can lead to an upregulated expression of immediate early genes (IEGs) in brain regions where the seizures develop,³⁵ we measured the expression of an IEG, *fosab*, at 3 dpf and 5 dpf by performing qPCR on cDNA obtained from larvae

heads. Compared to WTs, *kcna1a*^{-/-} larvae brains showed a significant upregulation in the *fosab* transcript levels at 3 dpf and 5 dpf, another confirmation of brain hyperexcitability (Figure 4E). Other zebrafish epilepsy models show disruption in the neuronal excitatory/inhibitory (E/I) balance.^{36,37} Thus we quantified excitatory glutamatergic (*vglut2a*) and inhibitory GABAergic (*gad1b*) neuronal marker expression in the larval brains by performing qPCR at 3 dpf and 5 dpf. The expression of *vglut2a* was significantly upregulated; however, *gad1b* transcript levels were significantly reduced in *kcna1a*^{-/-} larvae compared to WTs at 3 dpf and 5 dpf, indicative of excitatory/inhibitory (E/I) imbalance in neurons due to mutation in *kcna1a* (Figure 4F,G).

3.5 | *kcna1a*^{-/-} larvae experience compromised mitochondrial health

Studies on cortical cell cultures generated from epileptic rodent brains demonstrate that prolonged seizure activity negatively affects mitochondrial bioenergetics and induces cell death.³⁸ Our group and others show that mitochondrial bioenergetics is altered in various epileptic models of zebrafish.^{24,39,40} Here, we used the Seahorse XF Flux Bioanalyzer to assess whether mitochondrial bioenergetics is dysregulated in our *kcna1a*^{-/-} larvae at 3 dpf and 6 dpf (Figure 5A). We found that basal respiration was significantly decreased in *kcna1a*^{-/-} larvae at 3 dpf and 6 dpf compared to WTs (Figure 5B). Moreover, a significant reduction in mitochondrial respiration at 6 dpf (unchanged at 3 dpf) and a significant reduction in non-mitochondrial respiration at 3 dpf (unchanged at 6 dpf) in *kcna1a*^{-/-} larvae compared to WTs (Figure 5C,D)

was observed. These findings collectively indicate that *kcna1a*^{-/-} larvae experience decreased energy utilization, which is consistent with brain positron emission tomography (PET) scan findings in a patient with EA1 due to *KCNA1* mutation.⁴¹

4 | DISCUSSION

Currently, there are no standard treatment options for patients with EA1. In this study, we generated and characterized a *kcna1a* loss-of-function zebrafish model of EA1 with epilepsy. Notably, these zebrafish mutants were responsive to the existing first-line treatment of carbamazepine, suggesting clinical translation of this model. We propose that this *kcna1a*^{-/-} zebrafish model can be employed to further study the underlying biology of this disorder as well as for future drug screening to identify effective therapies.

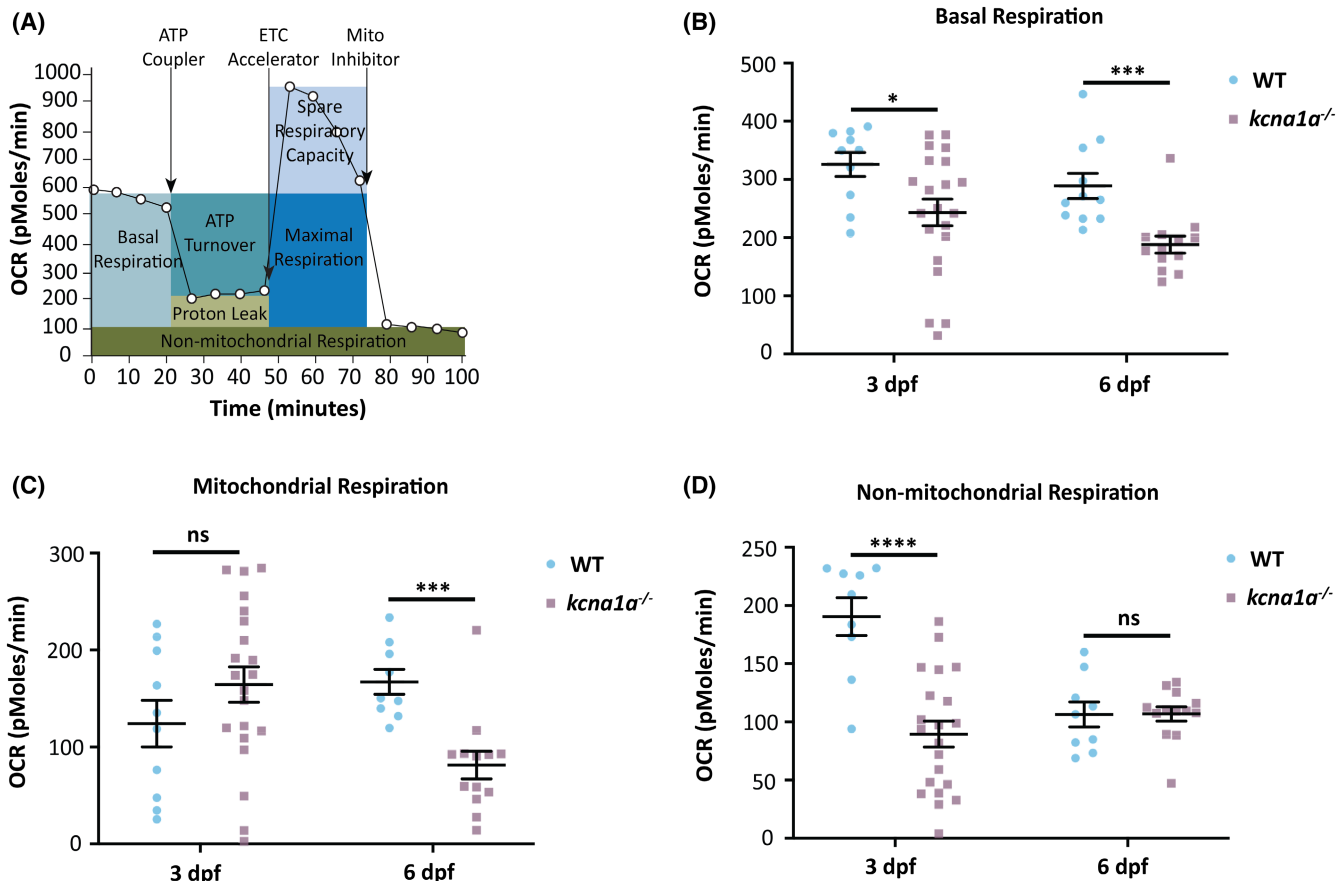


FIGURE 5 Metabolic characterization of *kcna1a*^{-/-} zebrafish. (A) Schematic representation of how the Seahorse bioanalyzer displays mitochondria bioenergetics as regulated by pharmacological inhibitors. (B) Quantification of basal respiration. *kcna1a*^{-/-} exhibit a significant reduction in basal respiration compared to WT at 3 dpf and 6 dpf. WT, *n* = 10; *kcna1a*^{-/-}, *n* = 21 at 3 dpf. WT, *n* = 11; *kcna1a*^{-/-}, *n* = 13 at 6 dpf. (C) Quantification of mitochondrial respiration. *kcna1a*^{-/-} exhibit a significant reduction in mitochondrial respiration compared to WT at 6 dpf. WT, *n* = 10; *kcna1a*^{-/-}, *n* = 21 at 3 dpf. WT, *n* = 9; *kcna1a*^{-/-}, *n* = 13 at 6 dpf. (D) Quantification of non-mitochondrial respiration. *kcna1a*^{-/-} exhibit a significant reduction in non-mitochondrial respiration compared to WT at 3 dpf. WT, *n* = 19; *kcna1a*^{-/-}, *n* = 21 at 3 dpf. WT, *n* = 9; *kcna1a*^{-/-}, *n* = 13 at 6 dpf. Data are mean ± SEM, ns: no significant changes observed, **p* ≤ .05, ****p* ≤ .001, *****p* ≤ .0001 - Unpaired *t* test. OCR, oxygen consumption rate.

To date, *KCNA1* is the only gene associated with EA1, with more than 40 *KCNA1* loss-of-function missense mutations reported.^{7,42} Although a range of symptoms are caused by variants in *KCNA1*, half of the patients are diagnosed with EA1 singly, and the other half are diagnosed with EA1 plus one or more associated comorbidities, such as epilepsy, myokymia, hyperthermia, hypomagnesemia, and/or scoliosis.^{4,11,43,44} Predictably, patients with distinct *KCNA1* variants have differential responses to drug treatments, recently confirmed by a report compiled from the available clinical findings of 15 patients with 36 treatment efforts using 12 different drugs.¹⁰ The authors found that two sodium channel blockers were promising, with carbamazepine the most therapeutically beneficial and phenytoin causing substantial clinical improvement. Acetazolamide displayed a mixed response, with ~45% patients showing positive effects but the majority without any improvement. Another sodium channel blocker, lamotrigine, was also found to be effective in controlling seizure episodes in a study.¹¹ Currently, the field lacks a model system that accurately phenocopies the patient and that can be robustly employed in large-scale screening for new drugs. We propose that our *kcna1a*^{-/-} zebrafish are a useful model to study etiology and for the identification of new treatment options for individuals that harbor a *KCNA1* mutation.

We previously used *kcna1a* zebrafish morphants to test our neurometabolism-focused anti-seizure drug screening platform. *kcna1a* morphants demonstrate hyperactivity when tracked in the dark, as well as ~70% of morphants show brain hyperexcitability in extracellular field recordings. Among several compounds screened, Vorinostat, a histone deacetylase inhibitor, was selected as a candidate drug for treating epilepsy as it significantly restores dysregulated bioenergetics parameters and reduces brain hyperexcitability in *kcna1a* morphants.²⁴ Our present study describes a new zebrafish *kcna1a*^{-/-} model that recapitulates many aspects of EA1 and epilepsy observed in patients with *KCNA1* mutations. Our zebrafish *kcna1a*^{-/-} larvae show dynamic behavioral deficits, with enhanced swimming activity in early stages and reduced swimming activity with uncoordinated movement at later stages of development (indicative of ataxia). Similar abnormal swimming patterns have been reported in another zebrafish model of ataxia.⁴⁵ Furthermore, the presence of hyperexcitability and bursting in extracellular field recordings, along with upregulated mRNA expression of *fosab* and perturbed E/I balance, is consistent with an epilepsy phenotype in these mutants. Due to its reported expression in the interneurons, *KCNA1* loss-of-function mutations result in impaired inhibitory synapse transmission, thereby enhancing brain hyperexcitability in the form of spontaneous seizures.^{6,46} Thus, we speculate

that the loss of Kcna1 potassium channel function in our zebrafish mutants possibly results in an alteration in E/I neurotransmission balance that ultimately leads to spontaneous epileptiform discharges in the brain. In addition, the early death of our *kcna1a*^{-/-} zebrafish correlates with sudden unexpected death in epilepsy (SUDEP), which also occurs in neuron-specific *Kcna1* knockout mice.⁴⁷ The abnormal startle behavior exhibited by *kcna1a*^{-/-} larvae mimics the spasms triggered by EA1 patients in response to external stimuli. Similar deficits in acoustic startle response and habituation learning have been reported in other *kcna1a*^{-/-} zebrafish models.^{31,48} It is intriguing that we found that the impaired startle response of our *kcna1a*^{-/-} zebrafish is normalized by three medications (acetazolamide, phenytoin, and lamotrigine), which also show some positive effects on patients with EA1. Moreover, treatment with the first-line therapy, carbamazepine, in *kcna1a*^{-/-} zebrafish rescues the impaired startle response along with the epileptiform discharges, whereas treatment in *Kcna1*^{-/-} mice had no effect on seizure frequency, indicating that *kcna1a*^{-/-} zebrafish might better phenocopy EA1 patients, at least in their responsiveness to this therapeutic. Carbamazepine is a promising drug for individuals with EA1 and epilepsy due to its improved tolerability when used chronically. Thus we focused our study herein on carbamazepine because it is more likely to be a primary therapy in patients and, therefore, serves as a better test candidate to demonstrate translatability of our zebrafish model. Notably, the other compounds, that is, acetazolamide, phenytoin, and lamotrigine, are either unsafe for long-term use due to multiple side-effects or lack evidence of robust clinical efficacy, making additional testing on these drugs needed but beyond the scope of this study.

Our bioenergetics analyses show that the *kcna1a*^{-/-} zebrafish exhibit a significant reduction in neurometabolism. Of interest, we previously observed opposite OCR effects in the *kcna1a* morpholino-injected larvae, whereby an increase in basal respiration, total mitochondrial respiration, and ATP-linked respiration is observed.²⁴ These differences could be due to variability in the epilepsy models used, that is, acute *kcna1a* morphants that disrupt this potassium channel during development vs chronic spontaneous seizures that arise from persistent *kcna1a* loss-of-function. Such differences in patterns of metabolic deficits have also been reported previously using other zebrafish models of epilepsy.⁴⁰ Ultimately, regardless of whether the bioenergetics outputs are increased or decreased in the *kcna1a* morphants vs *kcna1a*^{-/-} genetic mutants, mitochondrial function is compromised in both models.

It is important to note that our *kcna1a*^{-/-} zebrafish are a promising model for drug screening as well as extensive transcriptomic/proteomics profiling for gaining

new insights into the molecular pathways behind this disorder. Several research groups show that drugs that are functional in humans have a same target in zebrafish, including targeted cancer therapies like mitogen-activated protein kinase (MAPK)/extracellular signal-regulated kinase (ERK) kinase (MEK) inhibitors⁴⁹ and serotonin modulators.³⁴ More than two decades of zebrafish research in drug screening suggests that most molecules that are active in zebrafish are also active in humans and rodents.^{50,51} Thus zebrafish hold the potential to be extensively utilized for drug repurposing and precision medicine-based drug discovery.

The field can further benefit by generating new *kcna1a* loss-of-function zebrafish models recapitulating patients' mutations to unravel the differentially regulated signaling pathways as well as to compare their responsiveness to different drug treatments. Precision gene editing can help generate patient-specific models in zebrafish, and these models can recapitulate the etiology found in the patients.⁵² We must, however, remember the shortcomings of using zebrafish as a model system in isolation, including the absence of corticospinal and rubrospinal tracts in the zebrafish central nervous system (CNS)⁵³ and gene duplication leading to genetic redundancy that could complicate model development.⁵⁴ Therefore, efforts should be made to incorporate other model systems such as rodents and/or patient-derived brain organoids⁵⁵ to further validate top drug candidates from a zebrafish-based drug screening before they reach clinical trials.

5 | CONCLUSIONS

Here, *kcna1a*^{-/-} larvae recapitulate several phenotypes observed in the patient, including ataxia, epilepsy, and locomotion behavioral deficits. In addition, the observation that these zebrafish mutants are responsive to carbamazepine treatment similar to EA1 patients shows a translation of this EA1 model. Our study supports the notion that zebrafish epilepsy models are valuable for drug screening and suitable for both testing new therapeutical approaches and dissecting the underlying etiology of this disorder.

AUTHOR CONTRIBUTIONS

Deepika Dogra designed the study, performed the experiments, analyzed the data, and wrote the manuscript; Paola L. Meza-Santoscoy designed some experiments, and performed some of the behavioral assays and in situ hybridization experiments; Renata Rehak generated the zebrafish mutants and performed some of the mice experiments; Cristiane L. R. de la Hoz performed some of the mice experiments; Kingsley Ibhazehiebo performed

bioenergetics experiments; Cezar Gavrilovici and Jong M. Rho planned and performed electrophysiological experiments; Deborah M. Kurrasch designed the study, analyzed the data, wrote the manuscript, and supervised the work. All the authors commented on the manuscript.

ACKNOWLEDGMENTS

We would like to thank Dr. Timothy Simeone (Creighton University) for providing *Kcna1*^{+/-} breeders. We further thank Arthur Omorogiuwa and Natasha Klenin for assistance with zebrafish husbandry and genotyping. We also thank Elizabeth Hughes for assistance with mouse husbandry and genotyping and Younghee Ahn for training and support on the Seahorse XF Bioanalyzer. We thank Dr. Brian Ciruna and Denise Rebello for sharing the alizarin red staining protocol and helpful suggestions. Finally, we thank Alicia Vandenbrink for administrative support.

FUNDING INFORMATION


This project was funded by Brain Canada Platform Support Grant to D.M.K. and J.M.R.

CONFLICT OF INTEREST STATEMENT

D.M. Kurrasch and J.M. Rho are co-founders of Path Therapeutics, an early-stage biotech focused on the development of novel drugs for the treatment of Dravet syndrome. Their work with Path Therapeutics is not in conflict with the data presented herein. The other authors have nothing to disclose.

ORCID

Jong M. Rho  <https://orcid.org/0000-0001-9886-9924>

Deborah M. Kurrasch  <https://orcid.org/0000-0002-9945-287X>

REFERENCES

1. Rajakulendran S, Schorge S, Kullmann DM, Hanna MG. Episodic ataxia type 1: a neuronal potassium channelopathy. *Neurotherapeutics*. 2007;4(2):258–66.
2. Graves TD, Cha YH, Hahn AF, Barohn R, Salajegheh MK, Griggs RC, et al. Episodic ataxia type 1: clinical characterization, quality of life and genotype-phenotype correlation. *Brain*. 2014;137(Pt 4):1009–18.
3. Imbrici P, Altamura C, Gualandi F, Mangiatordi GF, Neri M, De Maria G, et al. A novel KCNA1 mutation in a patient with paroxysmal ataxia, myokymia, painful contractures and metabolic dysfunctions. *Mol Cell Neurosci*. 2017;83:6–12.
4. Kinali M, Jungbluth H, Eunson LH, Sewry CA, Manzur AY, Mercuri E, et al. Expanding the phenotype of potassium channelopathy: severe neuromyotonia and skeletal deformities without prominent episodic ataxia. *Neuromuscul Disord*. 2004;14(10):689–93.
5. Klein A, Boltshauser E, Jen J, Baloh RW. Episodic ataxia type 1 with distal weakness: a novel manifestation of a potassium channelopathy. *Neuropediatrics*. 2004;35(2):147–9.

6. Choi KD, Choi JH. Episodic ataxias: clinical and genetic features. *J Mov Disord*. 2016;9(3):129–35.
7. D'Adamo MC, Hasan S, Guglielmi L, Servettini I, Cenciarini M, Catacuzzeno L, et al. New insights into the pathogenesis and therapeutics of episodic ataxia type 1. *Front Cell Neurosci*. 2015;9:317.
8. Miceli F, Guerrini R, Nappi M, Soldovieri MV, Cellini E, Gurnett CA, et al. Distinct epilepsy phenotypes and response to drugs in KCNA1 gain- and loss-of function variants. *Epilepsia*. 2022;63(1):e7–e14.
9. Maggi L, Bonanno S, Altamura C, Desaphy JF. Ion Channel gene mutations causing skeletal muscle disorders: pathomechanisms and opportunities for therapy. *Cell*. 2021;10(6):1521.
10. Lauxmann S, Sonnenberg L, Koch NA, Bosselmann C, Winter N, Schwarz N, et al. Therapeutic potential of sodium channel blockers as a targeted therapy approach in KCNA1-associated episodic ataxia and a comprehensive review of the literature. *Front Neurol*. 2021;12:703970.
11. Rogers A, Golumbek P, Cellini E, Doccini V, Guerrini R, Wallgren-Pettersson C, et al. De novo KCNA1 variants in the PVP motif cause infantile epileptic encephalopathy and cognitive impairment similar to recurrent KCNA2 variants. *Am J Med Genet A*. 2018;176(8):1748–52.
12. Herson PS, Virk M, Rustay NR, Bond CT, Crabbe JC, Adelman JP, et al. A mouse model of episodic ataxia type-1. *Nat Neurosci*. 2003;6(4):378–83.
13. Begum R, Bakiri Y, Volynski KE, Kullmann DM. Action potential broadening in a presynaptic channelopathy. *Nat Commun*. 2016;7:12102.
14. Smart SL, Lopantsev V, Zhang CL, Robbins CA, Wang H, Chiu SY, et al. Deletion of the K(V)1.1 potassium channel causes epilepsy in mice. *Neuron*. 1998;20(4):809–19.
15. Rho JM, Szot P, Tempel BL, Schwartzkroin PA. Developmental seizure susceptibility of kv1.1 potassium channel knockout mice. *Dev Neurosci*. 1999;21(3–5):320–7.
16. Glasscock E, Yoo JW, Chen TT, Klassen TL, Noebels JL. Kv1.1 potassium channel deficiency reveals brain-driven cardiac dysfunction as a candidate mechanism for sudden unexplained death in epilepsy. *J Neurosci*. 2010;30(15):5167–75.
17. Aiba I, Noebels JL. Spreading depolarization in the brainstem mediates sudden cardiorespiratory arrest in mouse SUDEP models. *Sci Transl Med*. 2015;7(282):282ra46.
18. Simeone KA, Hallgren J, Bockman CS, Aggarwal A, Kansal V, Netzel L, et al. Respiratory dysfunction progresses with age in Kcna1-null mice, a model of sudden unexpected death in epilepsy. *Epilepsia*. 2018;59(2):345–57.
19. Dhaibar H, Gautier NM, Chernyshev OY, Dominic P, Glasscock E. Cardiorespiratory profiling reveals primary breathing dysfunction in Kcna1-null mice: implications for sudden unexpected death in epilepsy. *Neurobiol Dis*. 2019;127:502–11.
20. Thisse C, Thisse B. High-resolution in situ hybridization to whole-mount zebrafish embryos. *Nat Protoc*. 2008;3(1):59–69.
21. Stackley KD, Beeson CC, Rahn JJ, Chan SS. Bioenergetic profiling of zebrafish embryonic development. *PLoS One*. 2011;6(9):e25652.
22. Richon VM. Targeting histone deacetylases: development of vorinostat for the treatment of cancer. *Epigenomics*. 2010;2(3):457–65.
23. Baraban SC, Dinday MT, Castro PA, Chege S, Guyenet S, Taylor MR. A large-scale mutagenesis screen to identify seizure-resistant zebrafish. *Epilepsia*. 2007;48(6):1151–7.
24. Ibhazehiebo K, Gavrilovici C, de la Hoz CL, Ma SC, Rehak R, Kaushik G, et al. A novel metabolism-based phenotypic drug discovery platform in zebrafish uncovers HDACs 1 and 3 as a potential combined anti-seizure drug target. *Brain*. 2018;141(3):744–61.
25. Hortopan GA, Dinday MT, Baraban SC. Spontaneous seizures and altered gene expression in GABA signaling pathways in a mind bomb mutant zebrafish. *J Neurosci*. 2010;30(41):13718–28.
26. Brewster DL, Ali DW. Expression of the voltage-gated potassium channel subunit Kv1.1 in embryonic zebrafish Mauthner cells. *Neurosci Lett*. 2013;539:54–9.
27. Watanabe T, Shimazaki T, Mishiro A, Suzuki T, Hirata H, Tanimoto M, et al. Coexpression of auxiliary Kvbeta2 subunits with Kv1.1 channels is required for developmental acquisition of unique firing properties of zebrafish Mauthner cells. *J Neurophysiol*. 2014;111(6):1153–64.
28. Russo A, Gobbi G, Pini A, Moller RS, Rubboli G. Encephalopathy related to status epilepticus during sleep due to a de novo KCNA1 variant in the Kv-specific pro-Val-pro motif: phenotypic description and remarkable electroclinical response to ACTH. *Epileptic Disord*. 2020;22(6):802–6.
29. Chen H, von Hehn C, Kaczmarek LK, Ment LR, Pober BR, Hisama FM. Functional analysis of a novel potassium channel (KCNA1) mutation in hereditary myokymia. *Neurogenetics*. 2007;8(2):131–5.
30. Grone BP, Qu T, Baraban SC. Behavioral comorbidities and drug treatments in a zebrafish scn1lab model of Dravet syndrome. *eNeuro*. 2017;4(4):ENEURO.0066-17.2017.
31. Meserve JH, Nelson JC, Marsden KC, Hsu J, Echeverry FA, Jain RA, et al. A forward genetic screen identifies Dolk as a regulator of startle magnitude through the potassium channel subunit Kv1.1. *PLoS Genet*. 2021;17(6):e1008943.
32. Lavebratt C, Trifunovski A, Persson AS, Wang FH, Klason T, Ohman I, et al. Carbamazepine protects against megalencephaly and abnormal expression of BDNF and Nogo signaling components in the mceph/mceph mouse. *Neurobiol Dis*. 2006;24(2):374–83.
33. Deodhar M, Matthews SA, Thomas B, Adamian L, Mattes S, Wells T, et al. Pharmacoresponsiveness of spontaneous recurrent seizures and the comorbid sleep disorder of epileptic Kcna1-null mice. *Eur J Pharmacol*. 2021;913:174656.
34. Baraban SC, Dinday MT, Hortopan GA. Drug screening in Scn1a zebrafish mutant identifies clemizole as a potential Dravet syndrome treatment. *Nat Commun*. 2013;4:2410.
35. Morgan JI, Cohen DR, Hempstead JL, Curran T. Mapping patterns of c-fos expression in the central nervous system after seizure. *Science*. 1987;237(4811):192–7.
36. Brenet A, Hassan-Abdi R, Somkhit J, Yanicostas C, Soussi-Yanicostas N. Defective excitatory/inhibitory synaptic balance and increased neuron apoptosis in a zebrafish model of Dravet syndrome. *Cell*. 2019;8(10):1199.
37. Tiraboschi E, Martina S, van der Ent W, Grzyb K, Gawel K, Cordero-Maldonado ML, et al. New insights into the early mechanisms of epileptogenesis in a zebrafish model of Dravet syndrome. *Epilepsia*. 2020;61(3):549–60.

38. Kovac S, Domijan AM, Walker MC, Abramov AY. Prolonged seizure activity impairs mitochondrial bioenergetics and induces cell death. *J Cell Sci.* 2012;125(Pt 7):1796–806.
39. Kumar MG, Rowley S, Fulton R, Dinday MT, Baraban SC, Patel M. Altered glycolysis and mitochondrial respiration in a zebrafish model of Dravet syndrome. *eNeuro.* 2016;3(2):ENEURO.0008-16.201.
40. Banerji R, Huynh C, Figueroa F, Dinday MT, Baraban SC, Patel M. Enhancing glucose metabolism via gluconeogenesis is therapeutic in a zebrafish model of Dravet syndrome. *Brain Commun.* 2021;3(1):fcab004.
41. Kim JS, An JY, Lee KS, Chung YA, Choi JS, Lee KH. PET evidence of cerebellar hypometabolism in a patient with familial episodic ataxia-myokymia syndrome. *Mov Disord.* 2008;23(10):1483–5.
42. D'Adamo MC, Liantonio A, Rolland JF, Pessia M, Imbrici P. Kv1.1 channelopathies: pathophysiological mechanisms and therapeutic approaches. *Int J Mol Sci.* 2020;21(8):2935.
43. Browne DL, Gancher ST, Nutt JG, Brunt ER, Smith EA, Kramer P, et al. Episodic ataxia/myokymia syndrome is associated with point mutations in the human potassium channel gene, KCNA1. *Nat Genet.* 1994;8(2):136–40.
44. Paulhus K, Ammerman L, Glasscock E. Clinical spectrum of KCNA1 mutations: new insights into episodic ataxia and epilepsy comorbidity. *Int J Mol Sci.* 2020;21(8):2802.
45. Aspatwar A, Tolvanen ME, Jokitalo E, Parikka M, Ortutay C, Harjula SK, et al. Abnormal cerebellar development and ataxia in CARP VIII morphant zebrafish. *Hum Mol Genet.* 2013;22(3):417–32.
46. Thouta S, Zhang Y, Garcia E, Snutch TP. K(v)1.1 channels mediate network excitability and feed-forward inhibition in local amygdala circuits. *Sci Rep.* 2021;11(1):15180.
47. Trosclair K, Dhairbar HA, Gautier NM, Mishra V, Glasscock E. Neuron-specific Kv1.1 deficiency is sufficient to cause epilepsy, premature death, and cardiorespiratory dysregulation. *Neurobiol Dis.* 2020;137:104759.
48. Nelson JC, Witze E, Ma Z, Ciocco F, Frerotte A, Randlett O, et al. Acute regulation of habituation learning via posttranslational palmitoylation. *Curr Biol.* 2020;30(14):2729–38.e4.
49. Li D, March ME, Gutierrez-Uzquiza A, Kao C, Seiler C, Pinto E, et al. ARAF recurrent mutation causes central conducting lymphatic anomaly treatable with a MEK inhibitor. *Nat Med.* 2019;25(7):1116–22.
50. MacRae CA, Peterson RT. Zebrafish as tools for drug discovery. *Nat Rev Drug Discov.* 2015;14(10):721–31.
51. Afrikanova T, Serruys AS, Buenafe OE, Clinckers R, Smolders I, de Witte PA, et al. Validation of the zebrafish pentylentetrazol seizure model: locomotor versus electrographic responses to antiepileptic drugs. *PLoS One.* 2013;8(1):e54166.
52. Liu K, Petree C, Requena T, Varshney P, Varshney GK. Expanding the CRISPR toolbox in zebrafish for studying development and disease. *Front Cell Dev Biol.* 2019;7:13.
53. Babin PJ, Goizet C, Raldua D. Zebrafish models of human motor neuron diseases: advantages and limitations. *Prog Neurobiol.* 2014;118:36–58.
54. Howe K, Clark MD, Torroja CF, Torrance J, Berthelot C, Muffato M, et al. The zebrafish reference genome sequence and its relationship to the human genome. *Nature.* 2013;496(7446):498–503.
55. Samarasinghe RA, Miranda OA, Buth JE, Mitchell S, Ferando I, Watanabe M, et al. Identification of neural oscillations and epileptiform changes in human brain organoids. *Nat Neurosci.* 2021;24(10):1488–500.

SUPPORTING INFORMATION

Additional supporting information can be found online in the Supporting Information section at the end of this article.

How to cite this article: Dogra D, Meza-Santoscoy PL, Gavrilovici C, Rehak R, de la Hoz CLR, Ibhazehiebo K, et al. *kcna1a* mutant zebrafish model episodic ataxia type 1 (EA1) with epilepsy and response to first-line therapy carbamazepine. *Epilepsia.* 2023;64:2186–2199. <https://doi.org/10.1111/epi.17659>